Journal of Neurochemistry

JOURNAL OF NEUROCHEMISTRY | 2016

doi: 10.1111/jnc.13612

ORIGINAL ARTICLE

Protein interacting with NIMA (never in mitosis A)-1 regulates axonal growth cone adhesion and spreading through myristoylated alanine-rich C kinase substrate isomerization

Lucas J. Sosa,*,[2] James S. Malter,† Jie Hu,† Florentyna Bustos Plonka,‡ Mariana Oksdath,‡ Alvaro F. Nieto Guil,‡ Santiago Quiroga‡ and Karl H. Pfenninger*,[1]

*Department of Pediatrics and Colorado Intellectual and Developmental Disabilities Research Center, University of Colorado School of Medicine, Aurora, Colorado, USA

†Department of Pathology, University of Texas Southwestern Medical Center, Dallas, Texas, USA

‡Departamento de Química Biológica-CIQUIBIC, Facultad de Ciencias Químicas, Universidad Nacional de Córdoba-CONICET, Córdoba, Argentina

Abstract

Axonal growth cone motility requires precise regulation of adhesion to navigate the complex environment of the nervous system and reach its target. Myristoylated alanine-rich C kinase substrate (MARCKS) protein is enriched in the developing brain and plays an important, phosphorylation-dependent role in the modulation of axonal growth cone adhesion. The ratio of phospho-MARCKS (MARCKS-*P*) to total MARCKS controls adhesion modulation and spreading of the axonal growth cone. Pin1, a peptidyl-prolyl cis/trans isomerase (PPIase) that recognizes and binds to phosphorylated serine/threonine residues preceded by a proline (pSer/Thr-Pro) is also expressed in the developing brain. Here, we show that Pin1 is present in the growth cone, interacts with MARCKS-*P*, and regulates its dephosphorylation. We also described morphological alterations in the corpus callosum and cerebral cortex fibers of the Pin1 knockout mouse brain that may be caused by the misregulation of MARCKS-*P* and alterations of neuronal adhesion.

Keywords: brain development, corpus callosum, growth cone adhesion, isomerization, MARCKS, Pin1.

J. Neurochem. (2016) 10.1111/jnc.13612

The growth cone is a highly dynamic structure located at the tip of the neuronal axon which navigates in the complex environment of the central nervous system (CNS) to reach the appropriate target and establish precise connections (Kolodkin and Tessier-Lavigne 2011). The growth cone completes this complex function by sensing multiple types of guidance molecules (Dickson 2002; Kolodkin and Tessier-Lavigne 2011) and responds through the coordination of many cellular processes including cytoskeletal components, membrane trafficking, and the attachment and disassembly of the adhesion (Mortimer *et al.* 2008; Vitriol and Zheng 2012). Cell adhesions can modulate growth cone motility through engagement and coupling with the actin cytoskeleton, providing the force and traction necessary to drive the growth cone forward (clutch model) (Bard *et al.* 2008; Giannone *et al.* 2009; Lowery and Van Vactor 2009).

Myristoylated alanine-rich C kinase substrate (MARCKS) protein has been implicated in cell attachment, spreading, and motility (Manenti *et al.* 1997; Myat *et al.*

Received September 18, 2015; revised manuscript received January 20, 2016; accepted March 03, 2016.

Address correspondence and reprint requests to Lucas J. Sosa, Departamento de Química Biológica-CIQUIBIC, Facultad de Ciencias Químicas, Universidad Nacional de Córdoba-CONICET. Haya de la Torre esquina Medina Allende, Ciudad Universitaria, 5000 Córdoba, Argentina. E-mail: lucas@fcq.unc.edu.ar

[1]Dr Karl H. Pfenninger deceased January 30, 2015.

[2]Present address: Departamento de Química Biológica-CIQUIBIC, Facultad de Ciencias Químicas, Universidad Nacional de Córdoba-CONICET, Córdoba, Argentina

Abbreviations used: CNS, central nervous system; GCP, growth cone particles; MARCKS, myristoylated alanine-rich C kinase substrate; Pin1, protein interacting with NIMA (never in mitosis A)-1.

1997; Disatnik *et al.* 2004; Gatlin *et al.* 2006; Estrada-Bernal *et al.* 2009). MARCKS is highly expressed in the CNS (Albert *et al.* 1986; Blackshear *et al.* 1986; Ouimet *et al.* 1990; Lobach *et al.* 1993), it is enriched at the axonal growth cone (Katz *et al.* 1985; Mikule *et al.* 2003) where it helps regulate growth cone adhesion complexes (Gatlin *et al.* 2006), and is involved in axonal development (Xu *et al.* 2014). MARCKS expression is significantly higher in fetal than in adult rats brain (Patel and Kligman 1987) and it is required for brain development (Stumpo *et al.* 1995; Weimer *et al.* 2009). MARCKS contains a highly conserved, myristoylated N-terminal region and an effector domain susceptible to protein kinase C (PKC) mediated phosphorylation (Thelen *et al.* 1991; Kim *et al.* 1994; McLaughlin and Aderem 1995). MARCKS can also be phosphorylated by proline-directed protein kinases such as Cdk5 and MAPK (Taniguchi *et al.* 1994; Yamauchi *et al.* 1998; Ohmitsu *et al.* 1999). Although non-phosphorylated MARCKS is associated with the plasma membrane, stabilizing adhesion, whereas MARCKS-*P* translocates from the plasma membrane to the cytosol allowing detachment of adhesions (Thelen *et al.* 1991; Kim *et al.* 1994; Gatlin *et al.* 2006; Estrada-Bernal *et al.* 2009), little is known about the post-phosphorylation regulation of MARCKS and its effects on axonal growth cone adhesion and spreading.

Pin1 (protein interacting with NIMA (never in mitosis A)-1) is a peptidyl-prolyl *cis/trans* isomerase (PPIase) that specifically recognizes phosphorylated serine/threonine residues that immediately preceded to proline (pSer/Thr-Pro) and catalyzed the *cis/trans* isomerization of the intervening peptide bond (Lu *et al.* 1996; Ranganathan *et al.* 1997; Yaffe *et al.* 1997). The conformational changes in phosphorylated proteins isomerized by Pin1 control a variety of pathways and cellular functions (Liou *et al.* 2011). The isomerization of phosphorylated proteins by Pin1 can facilitate the action of phosphatases, affect protein stability or turnover, control the subcellular localization and enzymatic activities of proteins, and alter protein–protein interactions (Lu and Zhou 2007; Yeh and Means 2007; Takahashi *et al.* 2008; Liou *et al.* 2011). Pin1 is highly expressed in the CNS (Becker and Bonni 2006) and involved in neuronal differentiation (Nakamura *et al.* 2012), dendritic protein synthesis (Westmark *et al.* 2010), and axonal growth and guidance (Balastik *et al.* 2015). Although implicated in neurodegenerative diseases (Lu *et al.* 1999; Butterfield *et al.* 2006; Pastorino *et al.* 2006; Lu and Zhou 2007), little is known about Pin1′s physiological role during neurodevelopment. In this work we demonstrated that Pin1 binds to the (pSer/Thr-Pro) motif present in MARCKS-*P* and these interactions regulate the ratio of phosphorylated-to-unphosphorylated MARCKS that is essential for growth cone adhesion and function. We also demonstrated the presence of morphological alteration in the corpus callosum and the cerebral cortex fibers of the Pin1 knockout mice brain that may be mediated by the loss of regulation of MARCKS-*P*.

Materials and methods

Materials

The primary antibodies used and their sources were as follows: anti-MARCKS and anti-phospho-MARCKS, Santa Cruz Biotechnology, Inc. (Dallas, TX, USA); anti-phospho-MARCKS, Abcam PLC (Cambridge, MA, USA), for immunofluorescence ratio and pull-down experiment; anti-Pin-1, Abcam PLC, used for immunofluorescence and western blot; and anti-Actin, Sigma-Aldrich Co. LLC (St Louis, MO, USA), used for western blot. The secondary antibodies were as follows: anti-goat IgG conjugated with Alexa Fluor 594 (red); anti-rabbit IgG conjugated with Alexa Fluor 488 (green); anti-rabbit, anti-mouse, and anti-goat IgG conjugated with Alexa Fluor 647 (Cy5; for western blot), Life Co. (Carlsbad, CA, USA). The lipophilic tracer DiI (D282) from Life Co. was used to label the brain slice sections.

Reagents and their sources were as follows: TAT-His-WW-Pin1 is the 35 amino acid WW domain found at the N-terminus of Pin1 and fused to HIV TAT and poly-His purification tags. This peptide functions as a dominant negative (DN) to endogenous Pin1. TAT-His-green fluorescent protein (GFP) functions as a TAT control. Both were produced and used as described (Shen *et al.* 2009). The wtMARCKS construct was generated previously (Gatlin *et al.* 2006). Nerve growth factor, Alomone Labs (Jerusalem, Israel); fetal bovine serum, HyClone (Logan, UT, USA); tetradecanoyl phorbol acetate (TPA) from Sigma-Aldrich Co., LLC. Culture media, medium supplements, and laminin from Life Co. All other chemicals (highest quality available) were from Thermo-Fisher Scientific Inc. (Waltham, MA, USA) or Sigma-Aldrich Co., LLC.

Animals

Time-pregnant Sprague–Dawley rats were purchased from Harlan Sprague–Dawley Inc., Prattville, AL, USA, and maintained in an AAALAC-approved facility (Animal Welfare Assurance Number PHS A3269-01) and used in strict compliance with Protocol #B21711(01)1E (approved by the University of Colorado Denver's Animal Care and Use Committee), the US Public Health Service's Policy on Humane Care, and Use of Laboratory Animals and the Guide for the Care and Use of Laboratory Animals. Pin1 null mice and their control littermate brain tissue used to prepare the slice experiments were generously provided by James S. Malter.

Growth cone isolation

Axonal growth cones (GCPs) were isolated as described previously (Lohse *et al.* 1996; Pfenninger *et al.* 2003). Whole brains from fetal rats (18 days gestation) were homogenized in 0.32 M sucrose-containing 1 mM MgCl2, 2 mM TES buffer (2-[[1,3-dihydroxy-2-(hydroxymethyl)propan-2-yl]amino]ethanesulfonic acid), pH 7.3, and 2 μM aprotinin (all procedure at 4°C). Low-speed (1660 *g* for 15 min) supernatant of the homogenate was layered onto a discontinuous density gradient (0.83 and 2.66 M sucrose-containing 1 mM MgCl2 and 2 mM TES) and spun to equilibrium at 242 000 *g* at 4°C for 40 min in a vertical rotor (VTi50; Beckman

Coulter, Fullerton, CA, USA). GCPs were collected from the 0.32/0.83 M sucrose interface and then diluted with 0.32 M sucrose buffer, pelleted (40 000 *g* for 30 min), and then resuspended in an appropriate buffer depending on the subsequent experimentation.

Neuron culture and transfection

Hippocampal pyramidal neurons were dissociated from fetal E18 rat brain and plated onto laminin-coated glass coverslips (Assistant Brand; Carolina Biological Supply Co., Burlington, NC, USA). The cultures were maintained in Dulbecco's modified Eagle's medium plus N2 and B27 supplements, without serum (Bottenstein and Sato 1979) at 5% CO_2/37°C. For experiments requiring transfection, dissociated neurons were transfected prior to plating with wtMARCKS (5 μg of DNA) plus 1.5 μg pmaxGFP vector (to label the cells) or GFP alone in 100 μL of nucleofection reagent (Lonza Group Ltd, Basel, Switzerland). Transfection was carried out by electroporation, using the optimized Amaxa Nucleofector protocol (Lonza Group Ltd) for rat hippocampal neurons (setting O-003).

Dorsal root ganglion neurons were dissected from 15-day gestation Sprague–Dawley rat fetus, and cultured on laminin-coated coverslips in Neurobasal medium supplemented with B27, 10% v/v fetal bovine serum, and 100 ng/mL nerve growth factor (3.8 nM). After 24 h incubation at 5% CO_2/37°C, this medium was replaced with fresh Neurobasal medium plus B27, without other supplementation.

Fixation and immunofluorescence

Neurons were fixed using slow infusion of 4% Formaldehyde in 0.1 M phosphate buffer saline (PBS), pH 7.4, with 120 mM glucose and 0.4 mM CaCl2, as it was described (Pfenninger and Maylie-Pfenninger 1981). Cultures were rinsed (three times) with PBS containing 1 mM glycine, then they were permeabilized for 2 min with 1% (vol/vol) Brij98 detergent in blocking buffer [PBS, with 1% (wt/vol) bovine serum albumin] and placed in blocking buffer for 1 h at 25°C. Cultures were incubated with the primary antibodies with blocking solution for 3 h at 25°C. Then the cultures were rinsed three times with blocking buffer before adding the secondary antibodies [Alexa Fluor 594 (red) and Alexa fluor 488 (green)] for 1 h at 25°C. The secondary antibody was washed (3×) with blocking buffer before being mounted with Fluoromount-G (Southern Biotech, Birmingham, AL, USA) reagent.

Challenge experiments with peptides

Hippocampal neurons from fetal E18 rat brain were plated onto laminin-coated glass coverslips. After 24 h in culture, coverslips were mounted into an open chamber (Attofluor cell chamber, Molecular Probes/Life Co., Carlsbad, CA, USA) with medium, layered over with inert mineral oil (embryo-tested, sterile-filtered; Sigma-Aldrich Co. LLC) to maintain pH and avoid evaporation. They were then transferred to the microscope for live imaging under convective heating at 37°C. The neurons were challenged with 200 nM of TAT-His-WW-Pin1 (TAT-DN) or TAT-His-GFP (Ctrl) to the medium. After 10 min, phase contrast or reflection interference contrast microscopy (RICM) images were acquired from the same living growth cone. Growth cone area and accumulative close adhesion area were quantified by measuring the same live growth cone before and after treatment over a period of 10 min.

Cell viability assays

After 24 h in culture, hippocampal pyramidal neurons were challenged with 200 nM of TAT-His-WW-Pin1 (DN) or TAT-His-GFP (Ctrl) added to the medium. After 20 min, neuronal viability was determined by Trypan Blue exclusion. (Sosa *et al.* 2006).

Gel electrophoresis and western blot

Proteins were resolved by sodium dodecyl sulfate–polyacrylamide gel electrophoresis. After gel electrophoresis, the proteins were transferred to polyvinylidene difluoride membranes (Millipore Co., Billerica, MA, USA). The membranes were washed with Tris-buffered saline (TBS; 10 mM Tris pH 7.5, 150 mM NaCl) and then blocked for 1 h in non-fat milk and 0.1% Tween-20 in TBS (blocking buffer), incubated with primary antibody for at least 1 h (25°C), washed with TBS-Tween-20, incubated with Cy5 fluorophore-conjugated secondary antibody for 1 h, and washed. Bound antibody was acquired in a laser fluorescence scanner (Typhoon 9400; GE Healthcare, Piscataway, NJ, USA).

MARCKS-P/Pin1 co-immunoprecipitation

Fresh rats GCPs were resuspended in buffer (PBS, 1% Brij98, 1 μM ATP, and protease inhibitors) and treated with 1 μM of 12-*O*-tetradecanoyl-phorbol-13-acetate from Sigma-Aldrich Co., LLC, or vehicle for 3 min. To inhibit the reaction and solubilize the proteins, 1% of Tritron was added to the suspension and placed on ice for 10 min. The samples were spun at 18 500 g_{av} for 15 min to pellet undissolved proteins. The supernatant was collected and placed to incubate with 5 μg of antibodies overnight under agitation at 4°C. After this procedure, 100 μL of MagnaBind Protein G beads Thermo-Fisher Scientific Inc. were added to the suspension and incubated for 3 h under agitation at 4°C. The suspension was rinsed three times in PBS with a magnetic separator. Sodium dodecyl sulfate loading buffer was added to the beads and the sample analyzed by western blot.

GST pull-down assays

U251 cell line was harvested on cold PBS with inhibitor proteases. The cells were stimulated with TPA for 2 min at 25°C in 1% Brij98, 1 μM ATP, 10 mM HEPES, 1 mM MgCl, and 200 mM NaF. The reaction was inhibited by adding 10 nM of bisindolylmaleimide I (EMD Biosciences/Calbiochem, San Diego, CA, USA) on cold ice. The samples were spun at 18 500 g_{av} for 10 min to pellet undissolved proteins. The supernatant was collected and incubated with glutathione S-transferases proteins (GST) or GST-Pin1, plus Glutathione Magnetic Beads Thermo-Fisher Scientific Inc. for 2 h under agitation at 4°C. The suspension was rinsed three times in PBS with a magnetic separator and then loading buffer was added to the beads and the sample analyzed by western blot.

Brain slices section and labeling

To prepare brain slices, 60-day-old Pin1 −/− or their littermate control mice were under slow perfusion of 4% Formaldehyde in 0.1 M PBS, pH 7.4, with 120 mM glucose and 0.4 mM CaCl2 for 10 min. The fixed brains were remove and sectioned on a Microtome Cryostat HM 505E, Thermo-Fisher Scientific Inc. into 30 μm coronal sections. The slices were labeled with DiI crystals (D282) from Life Co. and incubated in the dark at 25°C for 10 min.

The slices were washed three times with PBS and then were embedded in Fluoromount-G (Southern Biotech) reagent. The samples were imaged 4 days after the procedure.

Microscopy

The *in vitro* images were acquired with a Zeiss Axiovert 200M microscope with Zeiss optics (objectives: Fluar 40x/1.3; Plan-Apo 63x/1.4; Alpha Plan-Apo 100x/1.46) (Carl Zeiss, Inc., Thornwood, NJ, USA) and Cooke Sensicam camera, controlled by μManager software (Edelstein *et al.* 2010). For live-cell imaging, cultures were placed in an open chamber with medium, layered over with inert mineral oil, and examined under convective heating (see above). Total areas of growth cone contact were determined in phase contrast. Adhesions were analyzed by RICM, which generates images based on the distance between the plasma membrane and the growth substratum (Izzard and Lochner 1976). Close adhesions were quantified using thresholding and area measurement (Metamorph software; Molecular Devices, LLC, Sunnyvale, CA, USA) (Sosa *et al.* 2013, 2014). The slices images at low magnification were acquired with an Olympus BX61 with an Olympus 4x/0.16 UPlan Sapo objective (Olympus Corporation, Tokio, Japan) and multiple image alignment was used to create photomicrographs of the brain. The slice images at higher magnification were taken using the inverted spinning disk confocal 3I Marianas (Intelligent Imaging Innovations, Inc., Denver, CO, USA) built around a Zeiss Axio Observer Z1 and equipped with Yokogawa CSU-X1 spinning disk unit (Yokogawa, Inc. Tokyo, Japan) and Evolve Photometrics EMCCD camera (Photometrics, Inc., Tucson, AZ, USA) with 512 × 512 resolution. The samples were imaged through a Zeiss EC Plan-Neofluar 40× NA = 1.3 oil objective (Carl Zeiss GmbH, Jena, Germany) using an excitation laser line of 561 nm and a bandpass emission filter 580–653 nm. To cover the whole area of interest 5 × 5 tiles (each tile image 170 × 170μm) or mosaic images were taken for each slide. To take into account all the cells in the whole tissue thickness z-stacks were taken spaced 1 μm apart and then collapsed in one image. The imaging acquisition and the stitching were done with Slidebook 5.5 imaging software (Intelligent Imaging Innovations, Inc.). Imaging experiments were performed in the University of Colorado Anschutz Medical Campus Advance Light Microscopy Core supported in part by NIH/NCATS Colorado CTSI Grant Number UL1 TR001082.

Statistical analysis

Data are presented as mean ± standard error of mean (SEM). Student's two-sample *t*-test was used to examine the statistically significant difference for two-group comparisons with a two-tailed distribution on samples. A value of $p \leq 0.05$ was considered statistically significant. n = number of neurons analyzed from at least two independent experiments. The growth cones colocalization were analyzed using ImageJ software and the JACoP plugging (National Institutes of Health, Rockville, MD, USA). The results were obtained with Costes' automatic threshold and Pearson's coefficient.

Results

Pin1 is present in the axonal growth cone of neurons and interacts with phosphorylated MARCKS

Previous reports described the presence of Pin1 in the neuronal nucleus, cytosol, dendrites (Lu *et al.* 1999; Becker and Bonni 2006; Westmark *et al.* 2010), and distal axon (Balastik *et al.* 2015). We thus determined if Pin1 is present in the axonal growth cone of developing neurons. To address this question, we performed immunofluorescence of hippocampal and dorsal root ganglion neurons in culture. We found high levels of Pin1 in the axonal growth cone, mainly distributed in the central region of the growth cone and the peripheral leading edge (Fig. 1a–b) where MARCKS and its phosphorylated form are also located (Fig. 1f–g) (Gatlin *et al.* 2006).

To confirm these data, western blot analysis of GCPs isolated from 18 days gestation rat brain demonstrated that

Fig. 1 Protein interacting with NIMA (never in mitosis A)-1 (Pin1) is enriched in hippocampal pyramidal growth cones and interacts with phosphorylated myristoylated alanine-rich C kinase substrate (MARCKS) in the axonal growth cone. (a) Immunofluorescence image of a hippocampal pyramidal neuron cultured on laminin and fixed after 24 h *in vitro*. The neuron was labeled with anti-Pin1 (green). Gc, axonal growth cone; pk, perikaryon. Scale bar, 20 μm. (b) Immunofluorescence image of the axonal growth cone of a dorsal root ganglion neuron cultured on laminin and fixed after 24 h *in vitro*. The growth cone was labeled with anti-Pin1 (green). Note the concentration of Pin1 along the leading edge of the growth cone. Scale bar, 20 μm. (c) Western blot of growth cone particles (GCPs) isolated from newborn rat brain probed for actin (Mr ~ 40) as a loading control and Pin1 (Mr ~ 16). Note the enrichment of Pin1 in the growth cone fraction (GCP) relative to brain homogenate (Hom) and low speed supernatant fraction (LSS), the parent fraction of GCPs. (d–e) Immunofluorescence image of a hippocampal pyramidal neuron (d) and an axonal growth cone (e) cultured on laminin and fixed after 24 h *in vitro*. The images were labeled with anti-MARCKS-*P* (green) and anti-Pin1 (red). Note the extensive colocalization (yellow) in the axonal growth cones in both figures. Scale bar, 20 μm (d) and 10 μm (e). Pearson's correlation $r = 0.72 \pm 0.03$ (values are mean ± SEM). $n = 11$. (f–g) Immunofluorescence image of a hippocampal pyramidal neuron (f) and an axonal growth cone (g) cultured on laminin and fixed after 24 h *in vitro*. The images were labeled with MARCKS (red) and anti-MARCKS-*P* (green). Scale bar, 20 μm (f) and 10 μm (g). (h) Growths cones isolated from 18 days gestation rat brain were treated with tetradecanoyl phorbol acetate (TPA) or vehicle and then probed for Pin1-phospho-Marcks binding after immunoprecipitation (IP). Quantification of Pin1 band intensity aisre shown at the bottom of the figure (arbitrary units; means ± SEM). Note the significant enrichment of Pin1 in the TPA-treated GCP compare to the not stimulate fraction. *p* value (Student's *t*-test, two-tailed analysis) (*$p \geq 0.001$). Data are representative of three independent experiments. (i) U251 cell extracts were treated with TPA (TPA input), incubated with GST-Pin1 or GST fusion protein, and then probed for MARCKS-*P* binding in immunoprecipitation (IP) experiments. MARCKS-*P* (Mr ~ 80) coprecipitated with GST-Pin1 but not with GST alone upon stimulation with TPA. Data are representative of two independent experiments. Quantification of MARCKS-*P* band intensity is shown at the bottom of the figure (arbitrary units; means ± SEM). *p* value (Student's *t*-test, two-tailed analysis) (*$p \geq 0.001$).

Pin1 is present and moderately enriched in the growth cone fraction in comparison with the homogenate and the low speed supernatant, the parent fractions of GCP (Fig. 1c). As Pin1 and MARCKS are both enriched in the axonal growth cone (Katz *et al.* 1985; Mikule *et al.* 2003) and MARCKS has several pSer/Thr-Pro motifs (Taniguchi *et al.* 1994; Yamauchi *et al.* 1998; Ohmitsu *et al.* 1999) that are potential recognition sites for Pin1, we hypothesized these two proteins interacted in the axonal growth cone. To test this, hippocampal neurons in culture were double immunolabeled using antibodies to Pin1 and phosphorylated MARCKS. We found a high level of protein colocalization at the axonal growth cone confirmed after a high Pearson's correlation R analysis ($r = 0.72 \pm 0.03$). The colocalization was found particularly in the central region and along the leading edge of the growth cone, where overlapping integrin/MARCKS

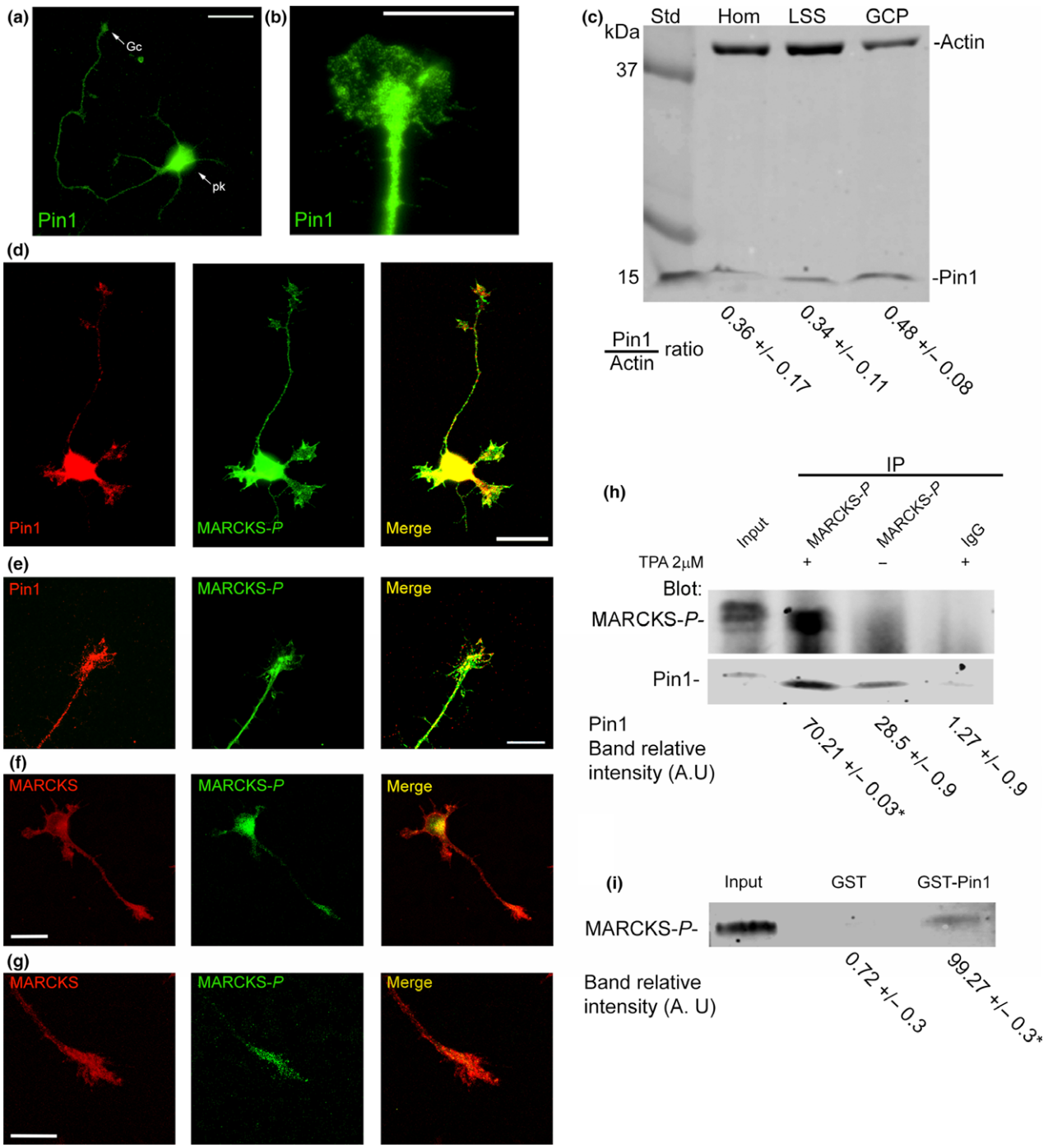

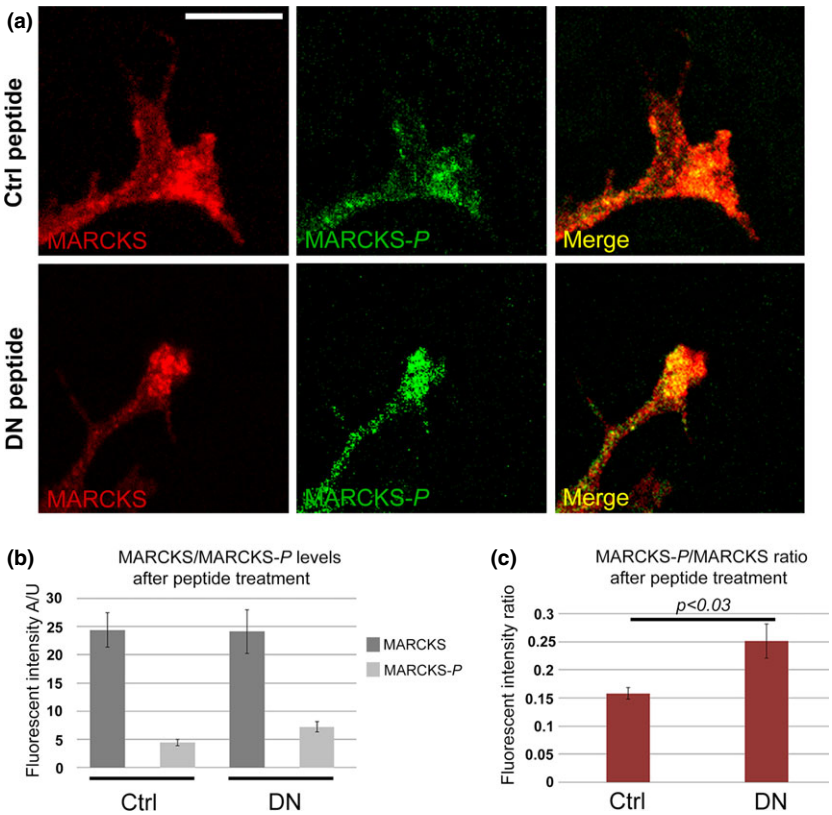

Fig. 2 Protein interacting with NIMA (never in mitosis A)-1 (Pin1) DN peptide increases the ratio of myristoylated alanine-rich C kinase substrate (MARCKS)-*P*/MARCKS. (a) Hippocampal pyramidal neurons were cultured on laminin. After 24 h *in vitro* they were challenged with 200 nM of Pin1 DN peptide or Ctrl peptide. Growth cones were labeled with anti-MARCKS (red) and anti-MARCKS-*P* (green) antibodies. In the merged image, overlap is yellow. Scale bar, 10 μm. (b) Bar graph shows average difference (± SEM) in fluorescent intensity (A/U) of MARCKS and MARCKS-*P* in the growth cone after 10 min of challenge with 200 nM Pin1 DN peptide (DN) or Ctrl peptide (Ctrl). Data are representative of three independent experiments. $n \geq 17$. (c) Bar graph shows fluorescent intensity ratio between MARCKS-*P* and MARCKS in the growth cone after 10 min of challenge with 200 nM Pin1 DN peptide (DN) or Ctrl peptide (Ctrl). Data are representative of three independent experiments. $n \geq 17$. *p* value (Student's *t*-test, two-tailed analysis).

was also described (Gatlin *et al.* 2006) (Fig. 1d–e). To further confirm these data, GCPs from embryonic rat brain were treated with either phorbol-12 myristate 13-acetate (TPA) (to stimulate the phosphorylation of MARCKS) (Estrada-Bernal *et al.* 2009) or vehicle prior to immunoprecipitation (IP) with anti-Pin1. The blot revealed increased MARCKS-*P* in the TPA-stimulated fraction and precipitated with Pin1 (Fig. 1h), whereas the GCPs treated with vehicle showed a weak band of MARCKS-*P* and a significantly reduced level of Pin1 (Fig. 1h). To confirm these results, we performed pull-down experiments with GST-Pin1. U251 cells were treated with TPA (TPA input) to enhance phosphorylated MARCKS. The extracts were then incubated with GST-Pin-1 fusion protein or GST as a control and then

Fig. 3 Protein interacting with NIMA (never in mitosis A)-1 (Pin1). Dominant negative peptide causes close adhesion detachment and growth cone collapse on laminin and this effect is rescued by wtMARCKS over-expression. Hippocampal pyramidal neurons were cultured on laminin. After 24 h *in vitro* they were challenged with 200 nM Pin1 DN peptide (DN) or Ctrl peptide (Ctrl). (a) Growth cone time-lapse series (phase contrast images). The numbers indicated minutes after addition of petide. Scale bar, 10 μm. Data are representative of three independent experiments. $n \geq 14$. (b) Reflection interference contrast microscopy (RCIM) images to show close adhesions (arrow heads, dark). The numbers indicated minutes after addition of peptides. Note the extensive growth cone collapse and close adhesion detachment caused by the DN Pin1 peptide (DN). Scale bar, 10 μm. Data are representative of three independent experiments. $n \geq 7$. (c) Hippocampal pyramidal neurons were transfected with wtMarcks plus green fluorescent protein (GFP) (wtMARCKS-GFP) or GFP vector only and cultured on laminin. After 24 h *in vitro* they were challenged with 200 nM of Pin1 DN peptide. Left, fluorescence images to identity-transfected growth cones. Scale bar, 20 μm. Right, RCIM time-lapse series of the same growth cones (green) after addition of the peptide. Note the extensive growth cone collapse and close adhesion detachment caused by the DN peptide in the Ctrl-GFP growth cone, but not after MARCKS transfection which rescue the phenotype. Scale bar, 10 μm. Data are representative of three independent experiments. $n \geq 9$. (d) Bar graph shows average difference (± SEM) in growth cone area (red bar graph) and cumulative close adhesion area (gray bar graph) after 10 min of challenge with the indicated peptides. *p* value (Student's *t*-test, two-tailed analysis). (e) Bar graph shows average difference (± SEM) on cell viability (determined by the criterion of Trypan Blue exclusion) of hippocampal pyramidal neurons after 10 min of treatment with 200 nM Pin1 DN peptide (DN) or Ctrl peptide (Ctrl). *n.s.,* not significant difference. Data are representative of three independent experiments. $n \geq 100$. (f) Bar graph shows average difference (± SEM) in growth cone close adhesion after 10 min of challenge with 200 nM Pin1 DN peptide (DN) in neurons transfected with wtMARCKS plus GFP or GFP alone. *p* value (Student's *t*-test, two-tailed analysis). MARCKS, myristoylated alanine-rich C kinase substrate.

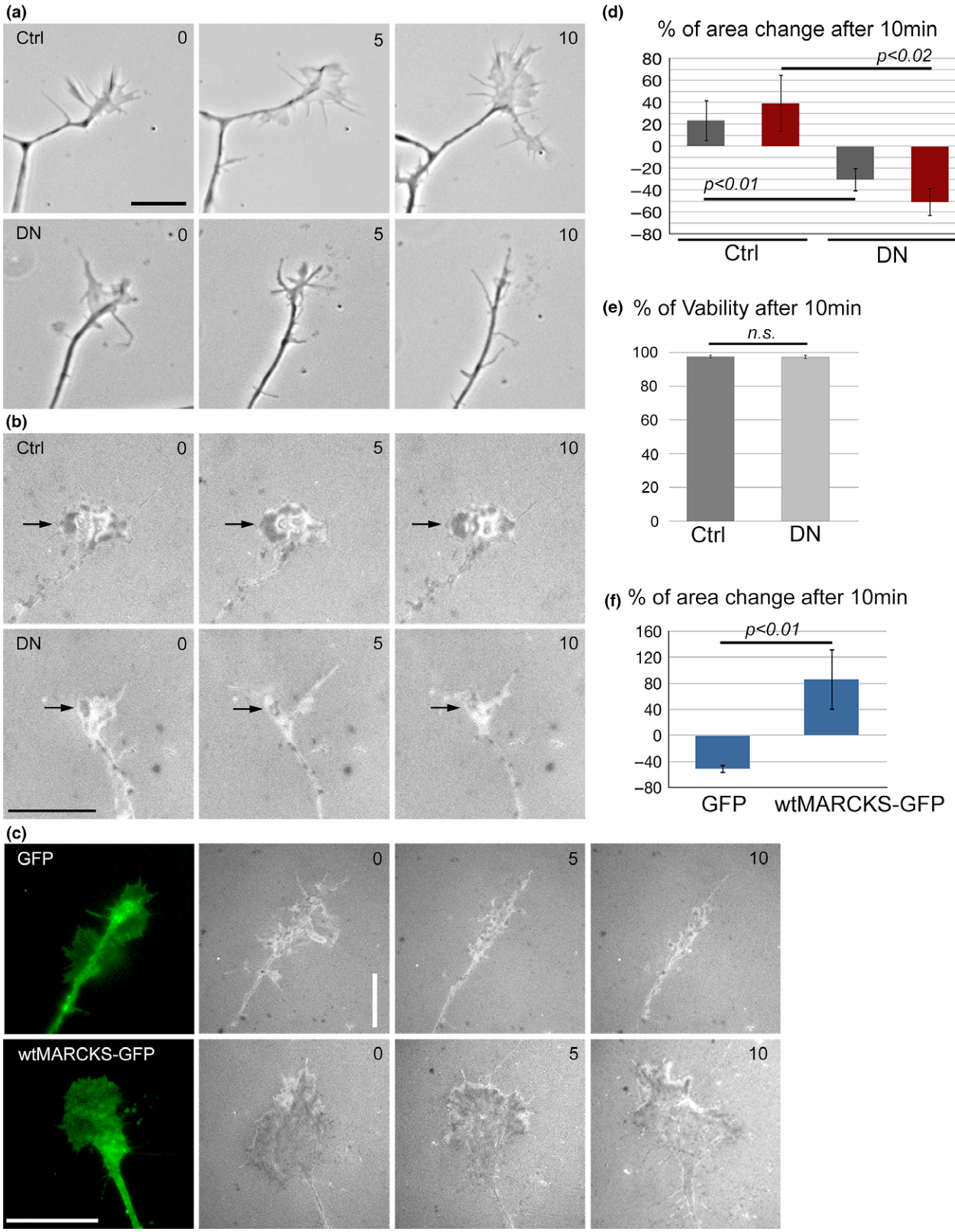
(a)
Ctrl
0
5
10
DN
0
5
10
(b)
Ctrl
0
5
10
DN
0
5
10
(c)
GFP
0
5
10
wtMARCKS-GFP
0
5
10
(d)
% of area change after 10min
p<0.02
p<0.01
80
60
40
20
0
−20
−40
−60
−80
Ctrl
DN
(e) % of Vability after 10min
n.s.
100
80
60
40
20
0
Ctrl
DN
(f) % of area change after 10min
p<0.01
160
120
80
40
0
−40
−80
GFP
wtMARCKS-GFP

probed for MARCKS-*P* binding by western blot. As shown (Fig. 1i), MARCKS-*P* (Mr ~ 80 KD) coprecipitated with GST-Pin1 but not with GST alone, further confirming the interaction of Pin1 with MARCKS-*P*.

Pin1 enhances phosphorylated MARCKS levels at the axonal growth cone

Pin-1 exerts its post-phosphorylation regulation of target proteins by *cis-trans* isomerization (Lu *et al.* 1996; Ranganathan *et al.* 1997; Yaffe *et al.* 1997). This conformational change often enhances the access to pSer or pThr by protein phosphatases (Zhou *et al.* 2000; Werner-Allen *et al.* 2011). Once dephosphorylated, the Ser/Thr-Pro peptide bond is effectively locked into a *trans* conformation. To address if Pin1 enhances the dephosphorylation of MARCKS, regulating the ratio of MARCKS-*P*/MARCKS, we performed immunofluorescence staining at the axonal growth cone of hippocampal neurons in cultures treated with either a Pin1 dominant negative (DN) peptide or a control. The N-terminal WW domain of Pin1 tethered to a TAT penetratin tag (TAT-His-WW-Pin1) (Shen *et al.* 2009) binds to Pin1 targets but lacks an isomerase domain, functioning as a dominant negative (TAT-DN). After incubation of neurons with TAT-DN peptide, MARCKS-*P* fluorescence intensity at the axonal growth cone was 1.6-fold greater than in neurons treated with TAT-GFP control (Fig. 2a-b). In cells treated with TAT-DN, the fluorescence intensity ratio between MARCKS-*P* and total MARCK in the growth cone had increased by 1.5-fold compared to TAT-GFP control or those treated with TPA alone (Fig. 2c). The level of total MARCKS was unchanged irrespective of treatment.

Pin-1 controls axonal growth cone spreading and close adhesion through MARCKS

MARCKS participates in neuronal spreading and migration and also stabilizes the adhesion complex at the growth cone (Manenti *et al.* 1997; Myat *et al.* 1997; Disatnik *et al.* 2004; Gatlin *et al.* 2006; Estrada-Bernal *et al.* 2009). Based on the interaction with and regulation of phospho-MARCKS, we speculated that Pin1 was involved in the modulation of the adhesions and the spreading of the axonal growth cone. To test this possibility, hippocampal neurons in culture were exposed to either TAT-DN or TAT-GFP control and phase contrast images taken after 10 min of the treatment. The growth cone of TAT-DN-treated neurons failed to spread and was significantly reduced in total area (Fig. 3a; bottom row and Fig. 3d; red bar graph) compared to TAT-GFP-treated control cells (Fig. 3a; top row and Fig. 3d; red bar graph).

To test if the contraction and deficient spreading of the axonal growth cones were a result of the reduction in attachment sites, RICM images were acquired from live axonal growth cones (Gatlin *et al.* 2006; Sosa *et al.* 2013, 2014) of neurons treated with either the TAT-DN or TAT-GFP peptides. The RICM method reveals close adhesions as dark areas, whereas wider contacts are brighter than the background (Izzard and Lochner 1976; Limozin and Sengupta 2009). The results of these experiments showed that the neurons treated with TAT-DN peptide exhibited a significant reduction in the accumulative close adhesion areas of the growth cone (Fig. 3b; bottom and Fig. 3d; gray bar graph). In contrast, the close adhesion of the axonal growth cone neurons treated with the control peptide were sustained over time and showed no significant changes (Fig. 3b; top and Fig. 3d; gray bar graph). To determine if the spreading deficiency and reduction in attachment sites of the axonal growth cones treated with TAT-DN peptide resulted from neuronal damage, we tested cell viability. The hippocampal neurons treated with the TAT-DN peptide showed no significant differences in viability by the criterion of Trypan Blue exclusion in comparison with those treated with the control peptide (Fig. 3e).

The TAT-WW DN peptide should inhibit many/all of the functions mediated by Pin1. To demonstrate that the observed alterations in growth cone function and size reflected increased amounts of MARCKS-*P,* hippocampal neuronal cultures were transfected with either wtMARCKS-GFP or GFP alone and challenged with the TAT-DN peptides. The neurons transfected only with GFP control constructs collapsed and lost the close adhesion sites at the axonal growth cone within 10 min of challenge with TAT-WW peptide (Fig. 3c; top row and Fig. 3f). In contrast, the neurons transfected with wtMARCKS-GFP were resistant to collapse or reductions in area despite treatment with TAT-DN peptides (Fig. 3c; bottom row and Fig. 3f). Therefore, we conclude that MARCKS is the target of Pin1 blockade and mediates growth cone stability and size as described in previous publications (Gatlin *et al.* 2006).

Pin-1 is involved in mouse brain development

The previous results showed that Pin1 is required for normal adhesion and spread of the axonal growth cone which is fundamental for axonal growth and guidance. These results imply that Pin1 is necessary for the normal development of the central nervous system and correct axonal connectivity *in vivo* (Kamiguchi 2007; Mortimer *et al.* 2008; Vitriol and Zheng 2012). Thus, we examined neuronal projections and morphology in the brain of conventional Pin1 knockout mice. Although cortical layer defects have been observed in Pin1 null mice (Nakamura *et al.* 2012), and developmental axon growth defects have been reported in the peripheral and CNS (Balastik *et al.* 2015), little is known about the status of neuronal projections in Pin1 null mice. To address this question we performed coronal brain sectioning of fixed Pin1 −/− or their WT littermates. We examined the corpus callosum (CC) which connects the two cortical hemispheres via a large axon bundle. This is where altered axonal outgrowth and path finding can be observed (Fenlon and Richards 2015). Pin1 −/− brain contained a thinner CC

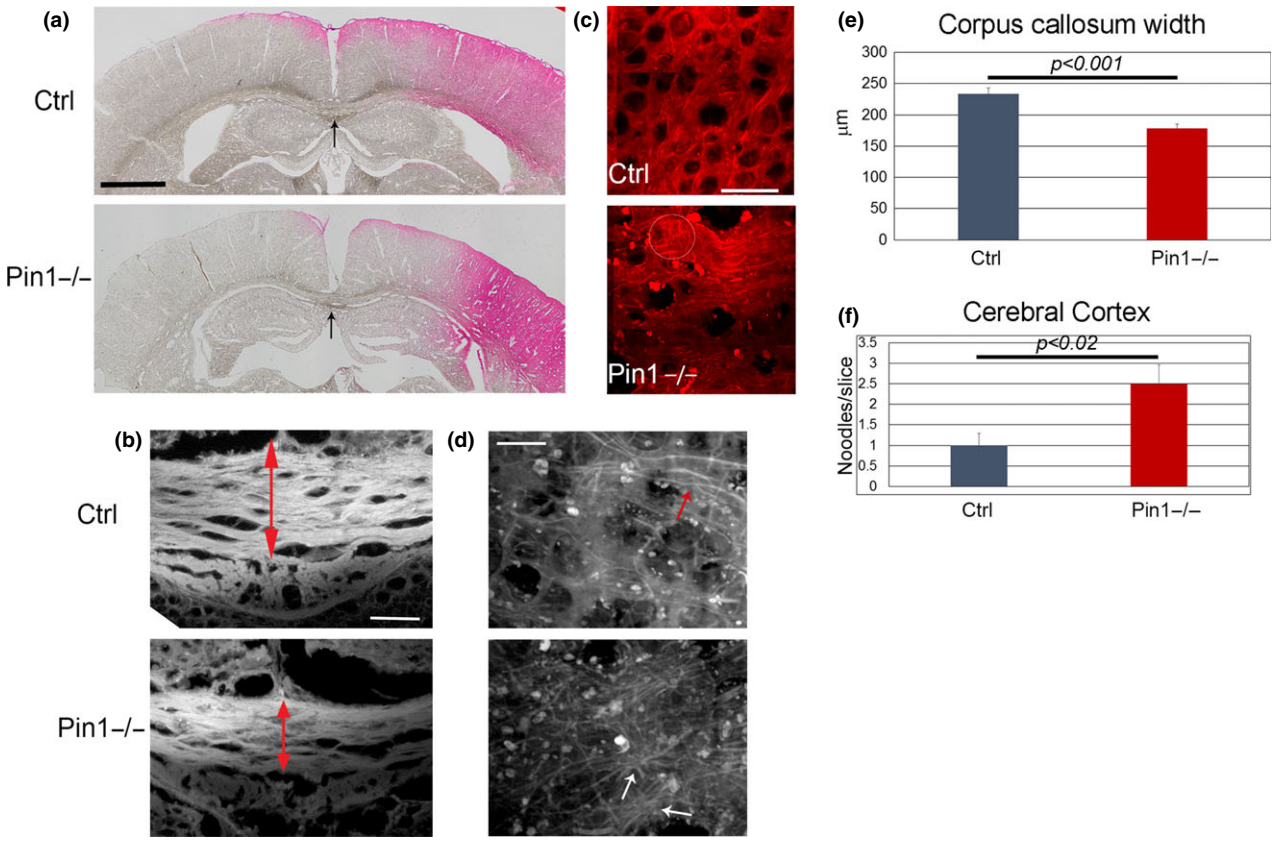

Fig. 4 Protein interacting with NIMA (never in mitosis A)-1 (Pin1) –/– deficit mice show reduced corpus callosum width and noodles disarranged fibers in the cerebral cortex. (a) Coronal brain section (30 µm) from Pin1 –/– or their Ctrl littermate mice labeled with DiI crystals is shown at low magnification (4×). Note the thinner Corpus Callosum (black arrows) present in the Pin1 –/– mice in comparison with their Ctrl. Scale bar, 1mm. (b) Higher magnification image (10×) from the Pin1 –/– or their Ctrl littermate mice Corpus Callosum labeled with DiI. Note the thinner Corpus Callosum (red arrows) present in the Pin1 –/– mice in comparison with their Ctrl. Scale bar, 100 µm. (c) Higher magnification image (40×) at the middle third of the cerebral cortex labeled with DiI. Note the presence of the disarranged fibers in the cerebral cortex of the Pin1 –/– mice (white circle). Scale bar, 50 µm. (d) Coronal brain section (30 µm) from Pin1 –/– or their Ctrl littermate mice labeled with DiI crystals are shown at higher magnification images (40×). Note the presence of the noodles disarranged fibers in the cerebral cortex of the Pin1 –/– mice (white arrows), whereas in the brain cortex of the Ctrl mice the fibers respect the pattern of orientation of the surrounding fibers (red arrow). Scale bar, 30 µm. (e) Bar graph shows average difference (+ SEM) in the Corpus Callosum width of Pin1 –/– mice (Pin1 –/–) (n = 6 slices, two mice) or their littermate Ctrl (Ctrl) (n = 6 slices, two mice). p value (Student's t-test, two-tailed analysis). (f) Bar graph shows average difference (+ SEM) in the numbers of tangles present in the cerebral cortex of Pin1 –/– mice (Pin1 –/–) (n = 6 slices, two mice) or their littermate Ctrl (Ctrl) (n = 6 slices, two mice). p value (Student's t-test, two-tailed analysis).

(black arrow-Fig. 4a; bottom and Fig. 4e) in the midline, with a reduction in the amount of fibers crossing over, compared with their littermate control mice (Fig. 4a; top and Fig. 4e). To confirm this feature, sections stained with DiI (Honig and Hume 1989; Lukas *et al.* 1998) and examined at higher magnification (10×) confirmed the development of a thinner CC in the Pin1 –/– brains (red double arrow – Fig. 4b; bottom and Fig. 4e) compared with their littermate control mice (red double arrow – Fig. 4b; top and Fig. 4e).

When we examined the status of neuronal projections at higher magnification (40×), the brain sections stained with DiI showed misarranged fibers or noodles among the projections from the cerebral cortex of the Pin1 –/– brains (white arrows and circle-Fig. 4c, d and f) mainly located in the middle third of the cerebral cortex. In contrast, the fibers of WT mice respected the pattern of orientation of the surrounding projections (red arrow – Fig. 4c, d and f).

Discussion

MARCKS is highly expressed in the developing brain that plays a critical role in the normal formation and patterning of the central nervous system (Stumpo *et al.* 1995). In neurons, MARCKS functions as an axonal growth cone adhesion

modulator. This function is dependent on the regulated phosphorylation (Gatlin *et al.* 2006) that drives MARCKS-*P* from the membrane to the cytoplasm with return to the membrane after dephosphorylation (Thelen *et al.* 1991; Kim *et al.* 1994; Gatlin *et al.* 2006; Estrada-Bernal *et al.* 2009). However, little is known about the proteins involved in the post-phosphorylation regulation of MARCKS and the potential effect of this post-transcriptional phenomenon on the axonal growth cone adhesion and spreading.

Pin1 is a peptidyl-prolyl isomerase that recognizes phosphorylated serine/threonine residues preceding a proline (pSer/Thr-Pro) and isomerizes from *cis* to *trans* the intervening peptide bond. The resulting conformational change alters protein location, signaling, and interactions (Lu and Zhou 2007; Liou *et al.* 2011). Although Pin1 has been implicated in the pathophysiology of Alzheimer disease through its interaction with and regulation of amyloid precursor protein cleavage and tau conformation (Lu *et al.* 1999; Butterfield *et al.* 2006; Pastorino *et al.* 2006), little is known about its physiological role in neurodevelopment. In this report we show that Pin1 is enriched at the axonal growth cone of developing neurons, distributed both in the central and peripheral regions, where the more dynamic adhesion sites are located (Estrada-Bernal *et al.* 2009). Pin1 localization was confirmed by western blot of GCPs. Based on these data we hypothesized a possible interaction with and regulation of MARCKS-*P*. MARCKS contains multiple Pin1-binding sites that are known to undergo cycles of phosphorylation/dephosphorylation. Indeed, IP's confirmed the interaction of Pin1 with MARCKS-*P* in the axonal growth cone of developing neurons. To determine the importance of these interactions on the fate of MARCKS-*P*, hippocampal neurons in culture were treated with a DN peptide composed of the N-terminal WW domain of Pin1 that lacks the isomerase domain. Multiple studies have shown that this peptide competitively prevents the interaction of endogenous Pin1 with its target (Shen *et al.* 2009; Westmark *et al.* 2010). In the functional absence of Pin1, the levels of MARCKS-*P* to total MARCKS significantly increased, suggesting Pin1-mediated isomerization was necessary prior to the dephosphorylation of MARCKS-*P* as has been described for other proteins (Zhou *et al.* 2000; Werner-Allen *et al.* 2011). Biologically, MARCKS-*P* was unable to recycle the plasma membrane, leading to destabilization of the adhesions of the axonal growth cone and reduced growth cone spreading (Gatlin *et al.* 2006) (Fig. 5).

These *in vitro* data predicted that Pin1 −/− mice should display abnormal white matter development. Indeed, Pin1 knockout mice showed significantly thinner corpus callosum than the control littermates as well as altered projection fibers in the middle third of the cerebral cortex. While cortical layer defects have been reported previously (Nakamura *et al.* 2012), these developmental anomalies can be explained by changes in the adhesion properties of the neuronal growth cone. Supporting this hypothesis are similar morphological alterations found in MARCKS null mice (Stumpo *et al.* 1995).

Consistent with our results, a recent publication described developmental axonal growth defects and perturbed guidance in Pin1 KO mice. These phenotypes were described to reduced stabilization of phosphorylated CRPMP2A by Pin1 and an increased susceptibility of the growth cone to collapse

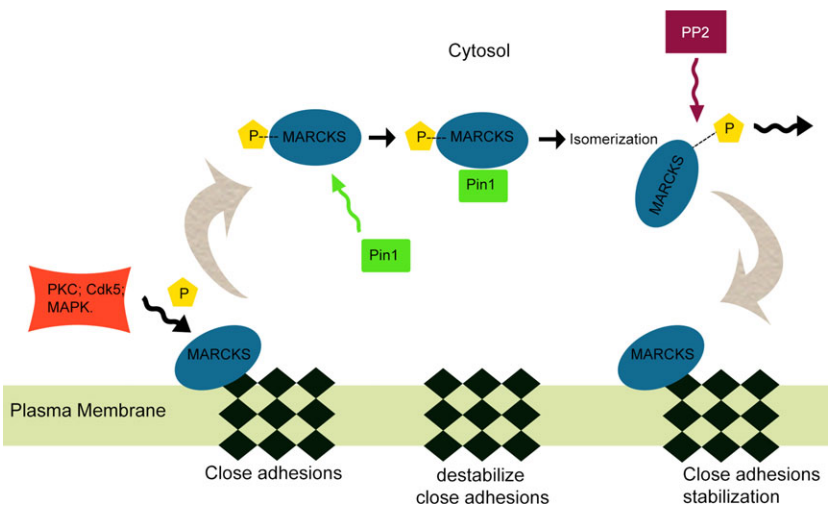

Fig. 5 PIn1-mediated myristoylated alanine-rich C kinase substrate (MARCKS) isomerization is required for growth cone recycling. MARCKS is found at the plasma membrane stabilizing the adhesion site of the growth cone. The phosphorylation of MARCKS by PKC or other kinases drive its returns to the cytoplasm (MARCKS-*P*). This dissociation of MARCKS from the plasma membrane causes adhesion weakness and growth cone detachment. Protein interacting with NIMA (never in mitosis A)-1 (Pin1) recognizes, binds, and isomerizes MARCKS-*P* in the cytosol, facilitating phosphatase action. The dephosphorylation of MARCKS allows it to return to the plasma membrane.

upon stimulation with Sema3A (Balastik *et al.* 2015). Interestingly, MARCKS phosphorylation is downstream and required for Sema3A to induced growth cone detachment and collapse (Gatlin *et al.* 2006).

In summary, we have shown that MARCKS, a critical factor in the directed movement of neuronal growth cones, is in turn regulated by both phosphorylation and *cis-trans* peptidyl isomerization mediated by Pin1. In the absence of Pin1, MARCKS is hyperphosphorylated, leading to loss of adhesions and collapse of the growth cone. As expected, major white matter tracks such as the corpus callosum are reduced in both Pin1 and MARCKS KO mice, consistent with control of the latter by the former.

Acknowledgments and conflict of interest disclosure

This study is dedicated to the memory of my mentor Dr Karl H. Pfenninger who passed away during the culmination of these studies. This work was supported by grants from International Society for Neurochemistry, CAEN Category 1C Return Home Grant 2014 to Lucas Javier Sosa (L.J.S), and Agencia Nacional de Promoción Científica y Tecnológica, Argentina, prestamo BID PICT 2014 No. 2331 (to L.J.S.) and PICT 2013 No. 1646 (to S.Q). These studies have also been supported by NIH HL088594 to J.S.M. The authors have no conflict of interest to declare.

References

Albert K. A., Walaas S. I., Wang J. K. and Greengard P. (1986) Widespread occurrence of "87 kDa", a major specific substrate for protein kinase C. *Proc. Natl Acad. Sci. USA* **83**, 2822–2826.

Balastik M., Zhou X. Z., Alberich-Jorda M. *et al.* (2015) Prolyl isomerase Pin1 regulates axon guidance by stabilizing CRMP2A selectively in distal axons. *Cell Rep.* **13**, 812–828.

Bard L., Boscher C., Lambert M., Mege R. M., Choquet D. and Thoumine O. (2008) A molecular clutch between the actin flow and N-cadherin adhesions drives growth cone migration. *J. Neurosci.* **28**, 5879–5890.

Becker E. B. and Bonni A. (2006) Pin1 mediates neural-specific activation of the mitochondrial apoptotic machinery. *Neuron* **49**, 655–662.

Blackshear P. J., Wen L., Glynn B. P. and Witters L. A. (1986) Protein kinase C-stimulated phosphorylation in vitro of a Mr 80,000 protein phosphorylated in response to phorbol esters and growth factors in intact fibroblasts. Distinction from protein kinase C and prominence in brain. *J. Biol. Chem.* **261**, 1459–1469.

Bottenstein J. E. and Sato G. H. (1979) Growth of a rat neuroblastoma cell line in serum-free supplemented medium. *Proc. Natl Acad. Sci. USA* **76**, 514–517.

Butterfield D. A., Abdul H. M., Opii W., Newman S. F., Joshi G., Ansari M. A. and Sultana R. (2006) Pin1 in Alzheimer's disease. *J. Neurochem.* **98**, 1697–1706.

Dickson B. J. (2002) Molecular mechanisms of axon guidance. *Science* **298**, 1959–1964.

Disatnik M. H., Boutet S. C., Pacio W., Chan A. Y., Ross L. B., Lee C. H. and Rando T. A. (2004) The bi-directional translocation of MARCKS between membrane and cytosol regulates integrin-mediated muscle cell spreading. *J. Cell Sci.* **117**, 4469–4479.

Edelstein A., Amodaj N., Hoover K., Vale R. and Stuurman N. (2010) Computer control of microscopes using μManager. *Curr. Protoc. Mol. Biol.* 14.20.1-14.20.17. doi: 10.1002/0471142727.mb1420s92

Estrada-Bernal A., Gatlin J. C., Sunpaweravong S. and Pfenninger K. H. (2009) Dynamic adhesions and MARCKS in melanoma cells. *J. Cell Sci.* **122**, 2300–2310.

Fenlon L. R. and Richards L. J. (2015) Contralateral targeting of the corpus callosum in normal and pathological brain function. *Trends Neurosci.* **38**, 264–272.

Gatlin J. C., Estrada-Bernal A., Sanford S. D. and Pfenninger K. H. (2006) Myristoylated, alanine-rich C-kinase substrate phosphorylation regulates growth cone adhesion and pathfinding. *Mol. Biol. Cell* **17**, 5115–5130.

Giannone G., Mege R. M. and Thoumine O. (2009) Multi-level molecular clutches in motile cell processes. *Trends Cell Biol.* **19**, 475–486.

Honig M. G. and Hume R. I. (1989) Dil and diO: versatile fluorescent dyes for neuronal labelling and pathway tracing. *Trends Neurosci.* **12**, 340–331.

Izzard C. S. and Lochner L. R. (1976) Cell-to-substrate contacts in living fibroblasts: an interference reflexion study with an evaluation of the technique. *J. Cell Sci.* **21**, 129–159.

Kamiguchi H. (2007) The role of cell adhesion molecules in axon growth and guidance. *Adv. Exp. Med. Biol.* **621**, 95–103.

Katz F., Ellis L. and Pfenninger K. H. (1985) Nerve growth cones isolated from fetal rat brain. III. Calcium-dependent protein phosphorylation. *J. Neurosci.* **5**, 1402–1411.

Kim J., Blackshear P. J., Johnson J. D. and McLaughlin S. (1994) Phosphorylation reverses the membrane association of peptides that correspond to the basic domains of MARCKS and neuromodulin. *Biophys. J.* **67**, 227–237.

Kolodkin A. L. and Tessier-Lavigne M. (2011) Mechanisms and molecules of neuronal wiring: a primer. *Cold Spring Harb. Perspect. Biol.* **3**, a001727.

Limozin L. and Sengupta K. (2009) Quantitative reflection interference contrast microscopy (RICM) in soft matter and cell adhesion. *ChemPhysChem* **10**, 2752–2768.

Liou Y. C., Zhou X. Z. and Lu K. P. (2011) Prolyl isomerase Pin1 as a molecular switch to determine the fate of phosphoproteins. *Trends Biochem. Sci.* **36**, 501–514.

Lobach D. F., Rochelle J. M., Watson M. L., Seldin M. F. and Blackshear P. J. (1993) Nucleotide sequence, expression, and chromosomal mapping of Mrp and mapping of five related sequences. *Genomics* **17**, 194–204.

Lohse K., Helmke S. M., Wood M. R., Quiroga S., de la Houssaye B. A., Miller V. E., Negre-Aminou P. and Pfenninger K. H. (1996) Axonal origin and purity of growth cones isolated from fetal rat brain. *Brain Res. Dev. Brain Res.* **96**, 83–96.

Lowery L. A. and Van Vactor D. (2009) The trip of the tip: understanding the growth cone machinery. *Nat. Rev. Mol. Cell Biol.* **10**, 332–343.

Lu K. P. and Zhou X. Z. (2007) The prolyl isomerase PIN1: a pivotal new twist in phosphorylation signalling and disease. *Nat. Rev. Mol. Cell Biol.* **8**, 904–916.

Lu K. P., Hanes S. D. and Hunter T. (1996) A human peptidyl-prolyl isomerase essential for regulation of mitosis. *Nature* **380**, 544–547.

Lu P. J., Wulf G., Zhou X. Z., Davies P. and Lu K. P. (1999) The prolyl isomerase Pin1 restores the function of Alzheimer-associated phosphorylated tau protein. *Nature* **399**, 784–788.

Lukas J. R., Aigner M., Denk M., Heinzl H., Burian M. and Mayr R. (1998) Carbocyanine postmortem neuronal tracing. Influence of different parameters on tracing distance and combination with immunocytochemistry. *J. Histochem. Cytochem.* **46**, 901–910.

Manenti S., Malecaze F. and Darbon J. M. (1997) The major myristoylated PKC substrate (MARCKS) is involved in cell spreading, tyrosine phosphorylation of paxillin, and focal contact formation. *FEBS Lett.* **419**, 95–98.

McLaughlin S. and Aderem A. (1995) The myristoyl-electrostatic switch: a modulator of reversible protein-membrane interactions. *Trends Biochem. Sci.* **20**, 272–276.

Mikule K., Sunpaweravong S., Gatlin J. C. and Pfenninger K. H. (2003) Eicosanoid activation of protein kinase C epsilon: involvement in growth cone repellent signaling. *J. Biol. Chem.* **278**, 21168–21177.

Mortimer D., Fothergill T., Pujic Z., Richards L. J. and Goodhill G. J. (2008) Growth cone chemotaxis. *Trends Neurosci.* **31**, 90–98.

Myat M. M., Anderson S., Allen L. A. and Aderem A. (1997) MARCKS regulates membrane ruffling and cell spreading. *Curr. Biol.* **7**, 611–614.

Nakamura K., Kosugi I., Lee D. Y., Hafner A., Sinclair D. A., Ryo A. and Lu K. P. (2012) Prolyl isomerase Pin1 regulates neuronal differentiation via beta-catenin. *Mol. Cell. Biol.* **32**, 2966–2978.

Ohmitsu M., Fukunaga K., Yamamoto H. and Miyamoto E. (1999) Phosphorylation of myristoylated alanine-rich protein kinase C substrate by mitogen-activated protein kinase in cultured rat hippocampal neurons following stimulation of glutamate receptors. *J. Biol. Chem.* **274**, 408–417.

Ouimet C. C., Wang J. K., Walaas S. I., Albert K. A. and Greengard P. (1990) Localization of the MARCKS (87 kDa) protein, a major specific substrate for protein kinase C, in rat brain. *J. Neurosci.* **10**, 1683–1698.

Pastorino L., Sun A., Lu P. J. *et al.* (2006) The prolyl isomerase Pin1 regulates amyloid precursor protein processing and amyloid-beta production. *Nature* **440**, 528–534.

Patel J. and Kligman D. (1987) Purification and characterization of an Mr 87,000 protein kinase C substrate from rat brain. *J. Biol. Chem.* **262**, 16686–16691.

Pfenninger K. H. and Maylie-Pfenninger M. F. (1981) Lectin labeling of sprouting neurons. II. Relative movement and appearance of glycoconjugates during plasmalemmal expansion. *J. Cell Biol.* **89**, 547–559.

Pfenninger K. H., Laurino L., Peretti D., Wang X., Rosso S., Morfini G., Caceres A. and Quiroga S. (2003) Regulation of membrane expansion at the nerve growth cone. *J. Cell Sci.* **116**, 1209–1217.

Ranganathan R., Lu K. P., Hunter T. and Noel J. P. (1997) Structural and functional analysis of the mitotic rotamase Pin1 suggests substrate recognition is phosphorylation dependent. *Cell* **89**, 875–886.

Shen Z. J., Esnault S., Schinzel A., Borner C. and Malter J. S. (2009) The peptidyl-prolyl isomerase Pin1 facilitates cytokine-induced survival of eosinophils by suppressing Bax activation. *Nat. Immunol.* **10**, 257–265.

Sosa L., Dupraz S., Laurino L., Bollati F., Bisbal M., Caceres A., Pfenninger K. H. and Quiroga S. (2006) IGF-1 receptor is essential for the establishment of hippocampal neuronal polarity. *Nat. Neurosci.* **9**, 993–995.

Sosa L. J., Bergman J., Estrada-Bernal A., Glorioso T. J., Kittelson J. M. and Pfenninger K. H. (2013) Amyloid precursor protein is an autonomous growth cone adhesion molecule engaged in contact guidance. *PLoS ONE* **8**, e64521.

Sosa L. J., Postma N. L., Estrada-Bernal A., Hanna M., Guo R., Busciglio J. and Pfenninger K. H. (2014) Dosage of amyloid precursor protein affects axonal contact guidance in Down syndrome. *FASEB J.* **28**, 195–205.

Stumpo D. J., Bock C. B., Tuttle J. S. and Blackshear P. J. (1995) MARCKS deficiency in mice leads to abnormal brain development and perinatal death. *Proc. Natl Acad. Sci. USA* **92**, 944–948.

Takahashi K., Uchida C., Shin R. W., Shimazaki K. and Uchida T. (2008) Prolyl isomerase, Pin1: new findings of post-translational modifications and physiological substrates in cancer, asthma and Alzheimer's disease. *Cell. Mol. Life Sci.* **65**, 359–375.

Taniguchi H., Manenti S., Suzuki M. and Titani K. (1994) Myristoylated alanine-rich C kinase substrate (MARCKS), a major protein kinase C substrate, is an in vivo substrate of proline-directed protein kinase(s). A mass spectroscopic analysis of the post-translational modifications. *J. Biol. Chem.* **269**, 18299–18302.

Thelen M., Rosen A., Nairn A. C. and Aderem A. (1991) Regulation by phosphorylation of reversible association of a myristoylated protein kinase C substrate with the plasma membrane. *Nature* **351**, 320–322.

Vitriol E. A. and Zheng J. Q. (2012) Growth cone travel in space and time: the cellular ensemble of cytoskeleton, adhesion, and membrane. *Neuron* **73**, 1068–1081.

Weimer J. M., Yokota Y., Stanco A., Stumpo D. J., Blackshear P. J. and Anton E. S. (2009) MARCKS modulates radial progenitor placement, proliferation and organization in the developing cerebral cortex. *Development* **136**, 2965–2975.

Werner-Allen J. W., Lee C. J., Liu P., Nicely N. I., Wang S., Greenleaf A. L. and Zhou P. (2011) cis-Proline-mediated Ser(P)5 dephosphorylation by the RNA polymerase II C-terminal domain phosphatase Ssu72. *J. Biol. Chem.* **286**, 5717–5726.

Westmark P. R., Westmark C. J., Wang S., Levenson J., O'Riordan K. J., Burger C. and Malter J. S. (2010) Pin1 and PKMzeta sequentially control dendritic protein synthesis. *Sci. Signal.* **3**, ra18.

Xu X. H., Deng C. Y., Liu Y. *et al.* (2014) MARCKS regulates membrane targeting of Rab10 vesicles to promote axon development. *Cell Res.* **24**, 576–594.

Yaffe M. B., Schutkowski M., Shen M. *et al.* (1997) Sequence-specific and phosphorylation-dependent proline isomerization: a potential mitotic regulatory mechanism. *Science* **278**, 1957–1960.

Yamauchi E., Kiyonami R., Kanai M. and Taniguchi H. (1998) The C-terminal conserved domain of MARCKS is phosphorylated in vivo by proline-directed protein kinase. Application of ion trap mass spectrometry to the determination of protein phosphorylation sites. *J. Biol. Chem.* **273**, 4367–4371.

Yeh E. S. and Means A. R. (2007) PIN1, the cell cycle and cancer. *Nat. Rev. Cancer* **7**, 381–388.

Zhou X. Z., Kops O., Werner A. *et al.* (2000) Pin1-dependent prolyl isomerization regulates dephosphorylation of Cdc25C and tau proteins. *Mol. Cell* **6**, 873–883.